Developmental Biology 434 (2018) 7–14

Contents lists available at ScienceDirect

Developmental Biology

journal homepage: www.elsevier.com/locate/developmentalbiology

Short Communication

Nr2f1a balances atrial chamber and atrioventricular canal size via BMP signaling-independent and -dependent mechanisms

Tiffany B. Duong[a,c], Padmapriyadarshini Ravisankar[c], Yuntao Charlie Song[b,c], Jacob T. Gafranek[b,c], Ariel B. Rydeen[b,c], Tracy E. Dohn[b,c], Lindsey A. Barske[e], J. Gage Crump[e], Joshua S. Waxman[c,d,*]

[a] Molecular and Developmental Biology Master's Program, University of Cincinnati College of Medicine, Cincinnati, OH, United States
[b] Molecular and Developmental Biology Graduate Program, University of Cincinnati College of Medicine, Cincinnati, OH, United States
[c] The Heart Institute and Molecular Cardiovascular Biology Division, Cincinnati Children's Hospital Medical Center, Cincinnati, OH, United States
[d] Developmental Biology Division, Cincinnati Children's Hospital Medical Center, Cincinnati, OH, United States
[e] Eli and Edythe Broad Center for Regenerative Medicine and Stem Cell Research, University of Southern California, Los Angeles, CA, United States

ARTICLE INFO

Keywords:
Nr2f1a
Zebrafish
Atrial myocardium
Atrioventricular canal
Valve development
Cardiac chambers

ABSTRACT

Determination of appropriate chamber size is critical for normal vertebrate heart development. Although Nr2f transcription factors promote atrial maintenance and differentiation, how they determine atrial size remains unclear. Here, we demonstrate that zebrafish Nr2f1a is expressed in differentiating atrial cardiomyocytes. Zebrafish *nr2f1a* mutants have smaller atria due to a specific reduction in atrial cardiomyocyte (AC) number, suggesting it has similar requirements to Nr2f2 in mammals. Furthermore, the smaller atria in *nr2f1a* mutants are derived from distinct mechanisms that perturb AC differentiation at the chamber poles. At the venous pole, Nr2f1a enhances the rate of AC differentiation. Nr2f1a also establishes the atrial-atrioventricular canal (AVC) border through promoting the differentiation of mature ACs. Without Nr2f1a, AVC markers are expanded into the atrium, resulting in enlarged endocardial cushions (ECs). Inhibition of Bmp signaling can restore EC development, but not AC number, suggesting that Nr2f1a concomitantly coordinates atrial and AVC size through both Bmp-dependent and independent mechanisms. These findings provide insight into conserved functions of Nr2f proteins and the etiology of atrioventricular septal defects (AVSDs) associated with *NR2F2* mutations in humans.

1. Introduction

The two fundamental subunits of the vertebrate heart, the atrial and ventricular chambers, receive and propel blood, respectively. Cardiomyocytes of the chambers differ in gene expression (Barth et al., 2005; DeLaughter et al., 2016; Li et al., 2016; McGrath and de Bold, 2009; Tabibiazar et al., 2003), reflecting requisite specialization in their cellular architecture and electrophysiological properties (Foglia et al., 2016; Gupta and Poss, 2012; Smyrnias et al., 2010). Mutations in genes that disrupt chamber development, including the transcription factors NKX2.5 and NR2F2 (aka Coupt-tfII) are associated with congenital heart defects in humans (Al Turki et al., 2014; Schott et al., 1998). Thus, establishment of normal relative chamber proportions is crucial for proper vertebrate heart development and function within the embryo and postnatally.

Although chamber progenitors distinguish themselves prior to gastrulation in vertebrate embryos (Abu-Issa and Kirby, 2008; Devine et al., 2014; Galli et al., 2008; Garcia-Martinez and Schoenwolf, 1993; Keegan et al., 2004; Stainier and Fishman, 1992; Waldo et al., 2005), it has become apparent that cardiomyocytes need to reinforce their chamber identity even after they are overtly differentiated (Bruneau et al., 2001; Koibuchi and Chin, 2007; Li et al., 2016; Pradhan et al., 2017; Targoff et al., 2013; Wu et al., 2013; Xin et al., 2007). Furthermore, factors that become specifically expressed in the atrial and ventricular cardiomyocytes (VCs) during development have been found to maintain chamber identity, rather than directly promote the specification of their progenitors. Recent work in zebrafish has indicated that Fgf8, which is specifically expressed in the ventricle (Reifers et al., 1998), lies at the top of a signaling network that reinforces ventricular identity upstream of Nkx2.5 (Pradhan et al., 2017). While Nkx2.5 is initially expressed broadly throughout cardiomyocyte progenitors and differentiating cardiomyocytes, studies in

* Corresponding author at: The Heart Institute and Molecular Cardiovascular Biology Division, Cincinnati Children's Hospital Medical Center, Cincinnati, OH, United States.
E-mail address: joshua.waxman@cchmc.org (J.S. Waxman).

https://doi.org/10.1016/j.ydbio.2017.11.010
Received 9 August 2017; Received in revised form 15 November 2017; Accepted 16 November 2017
Available online 20 November 2017
0012-1606/

both zebrafish and mice indicate that it has a conserved requirement maintaining VC identity at the expense of atrial identity through promoting the expression of the ventricle-specific genes *Irx4* and *Hey2* (Bruneau et al., 2001, 2000; Koibuchi and Chin, 2007; Li et al., 2016; Targoff et al., 2013, 2008; Xin et al., 2007). Conversely, members of the orphan nuclear hormone transcription factors Nr2f1 and Nr2f2 have expression restricted to atrial cardiomyocytes (ACs) in humans and mice and are required for proper atrial development (Devalla et al., 2015; Li et al., 2016; Pereira et al., 1999). Global mouse Nr2f2 KOs have smaller atria and sinus venosus (Pereira et al., 1999). However, following heart tube formation, conditional Nr2f2 KOs demonstrated that Nr2f2 is necessary and sufficient for maintaining atrial identity at the expense of ventricular identity through directly repressing *Irx4* and *Hey2* expression (Wu et al., 2013). Similarly, in human embryonic stem cell (hESC)-derived ACs, both Nr2f1 and Nr2f2 are required for AC differentiation and promote atrial-specific ion channel expression (Devalla et al., 2015). Importantly, genomic analysis in humans has associated mutations in NR2F2 with atrioventricular-septal defects (AVSDs) (Al Turki et al., 2014). However, despite the established requirements for Nr2f2 in atrial development and identity maintenance, previous studies have not provided insight into the mechanisms underlying the smaller atria in *Nr2f2* mouse mutants or *NR2F2*-associated AVSDs in humans.

In contrast to mice, zebrafish *nr2f2* mutants do not have early cardiovascular defects (van Impel et al., 2014), suggesting that other members of this highly conserved protein family may perform similar functions in zebrafish. Here, we demonstrate that zebrafish Nr2f1a is expressed specifically in cells adjacent to the venous atrial pole, which we postulate are putative AC progenitors, and ACs of the nascent heart tube. Functionally, we find that engineered *nr2f1a* mutants have smaller atria due to a reduction in the number of ACs, which differentiate more slowly at the venous pole. However, we also find that through promoting atrial differentiation at the atrial-atrioventricular canal (AVC) border Nr2f1a concomitantly determines the size of the AVC. *Nr2f1a* mutants have an expansion of AVC markers into the atrium, which ultimately leads to the differentiation of excess EC cells. Interestingly, inhibition of BMP signaling, an upstream determinant of AVC specification, can restore EC cell number, but not AC number. Thus, our data suggest that proper atrial chamber and AVC size are coordinated through Nr2f1a both promoting accrual of ACs at the venous pole independent of BMP signaling and establishing the atrial-AVC border through restricting BMP signaling. Our studies provide novel insight into the conserved mechanisms by which Nr2f members determine vertebrate atrial chamber and AVC size.

2. Materials and methods

2.1. Zebrafish line and maintenance

Adult zebrafish were raised and maintained under standard laboratory conditions. Transgenic lines used were *Tg(–5.1myl7:DsRed-NLS)* (Mably et al., 2003) and *Tg(myl7:Kaede)* (de Pater et al., 2009).

2.2. Generation of nr2f1a mutants

The *nr2f1a*^{el512} mutant allele was generated using TALENs targeting the 3′ end of exon 1: *nr2f1a* left TALEN: 5′-TGCCAATATTGT CGGCTGAA-3′, right TALEN: 5′-TATTCACCTTCCCGCCGCAT-3′. The TALEN plasmids were constructed by a PCR-based method (Sanjana et al., 2012) and linearized with *Stu*I (New England Biolabs). RNAs were synthesized with the mMessage Machine T7 Ultra kit (Ambion/ThermoFisher Scientific) and injected at 100 ng/μl into embryos at the 1 cell stage. Injected individuals were outcrossed to wild-type fish as adults, and the F1 progeny were screened for heterozygous mutations by restriction fragment length polymorphism assays. Mutant alleles predicted were identified by sequencing PCR products amplified with the following primers: *nr2f1a* F: 5′-CCTGCGAAGGATGCAAAAGT-3′ and *nr2f1a* R: 5′-TATATTCACCTTCCCGCCGC-3′. The *nr2f1a*^{el512} allele contains an 8-bp deletion resulting in a frameshift at the end of the DNA binding domain that terminates after the incorporation of 62 incorrect amino acids (Fig. 1D,E,F). The primers *nr2f1a* F1: GAGGA GTGTCCGAAGGAACTTA and *nr2f1a* R1: GAGGTCTGCATAAC CTTGCTTT were used for subsequent genotyping of the *nr2f1a*^{el512} allele.

The *nr2f1a*^{ci1009} allele was made using CRISPR/Cas9. The gene-specific sequence of the guide RNA (5′-GGCCAGTATGCGCTAACG AATGG) that targets a 5′ site of the *nr2f1a* 2nd exon was fused with the common portion using PCR and RNA was made using T7 as described previously (Talbot and Amacher, 2014). *Cas9* mRNA was made as described (Jao et al., 2013). 50 pg of the *nr2f1a* guide RNA was co-injected with 300 pg *cas9* mRNA. F1 progeny were screened using PCR for insertion and deletions using the primers *nr2f1a* e2-F1: 5′-TGGATGTACATTTCCTCTCCCT and *nr2f1a* e2-R1: 5′-CTGCA AGCTCACAGATGTTCTC. Bands predicted to have deletions were cloned and sequenced. An allele with a 49 bp deletion predicted to cause a truncation immediately after the ligand binding domain following 4 incorrect amino acids was found and subsequently recovered in the raised F1 generation (Fig. S2).

2.3. In situ hybridization (ISH) and length measurements

ISH was performed using NBT/BCIP (Roche) as previously reported (Oxtoby and Jowett, 1993). Digoxygenin-labeled anti-sense RNA probes for *amhc* (ZDB-GENE-031112-1), *vmhc* (ZDB-GENE-991123-5), *bmp4* (ZDB-GENE-980528-2059), *tbx2b* (ZDB-GENE-990726-27), *has2* (ZDB-GENE-020828-1), *notch1b* (ZDB-GENE-990415-183), *klf2a* (ZDB-GENE-011109-1), and *spp1* (ZDB-GENE-050706-97) were used. Length measurements of AVC markers were made using ImageJ by tracing the expression on the inferior side (adjacent to the outer curvature of the ventricle) and superior side (adjacent to the inner curvature) in frontal view images.

2.4. Real-time quantitative PCR (RT-qPCR)

Total RNA isolation and RT-qPCR was performed using previously reported methods (D'Aniello et al., 2013). Briefly, whole embryo RNA was obtained from groups of 30 embryos using Trizol (Ambion) and Purelink RNA Microkit (Invitrogen). cDNA was synthesized using 1 μg total RNA and the ThermoScript Reverse Transcriptase kit (Invitrogen). RT-qPCR was performed using Power SYBR Green PCR Master Mix (Applied Biosystems) in a BioRad CFX-96 PCR machine. Expression levels were standardized to *β-actin* expression and data were analyzed using the $2^{-\Delta\Delta CT}$ Livak Method. All experiments were performed in triplicate. Primer sequences for *β-actin, amhc,* and *vmhc* used in RT-qPCR were reported previously (D'Aniello et al., 2013; Rydeen et al., 2015).

2.5. Nr2f1a antibody

An affinity-purified rabbit polyclonal antibody was generated using a combination approach with the peptides QEDVAGGPPSGP NPAAQPAREQ (amino acids 12–33 of Nr2f1a) and QTPSQPGPP STPGTAGDKGSQNSGQSQ (amino acids 45–71 of Nr2f1a; Fig. S1) by YenZym Antibodies (www.YenZym.com).

2.6. Western blots

25 embryos per condition were harvested at 24 h post-fertilization (hpf) and were homogenized in embryo lysis buffer (20 mM Tris - pH8, 50 mM NaCl, 2 mM EDTA, 1% NP-40) with cOmplete™ protease inhibitor (Roche). Two embryo equivalents were run on a 10% polyacrylamide gel. Western blotting was performed using standard

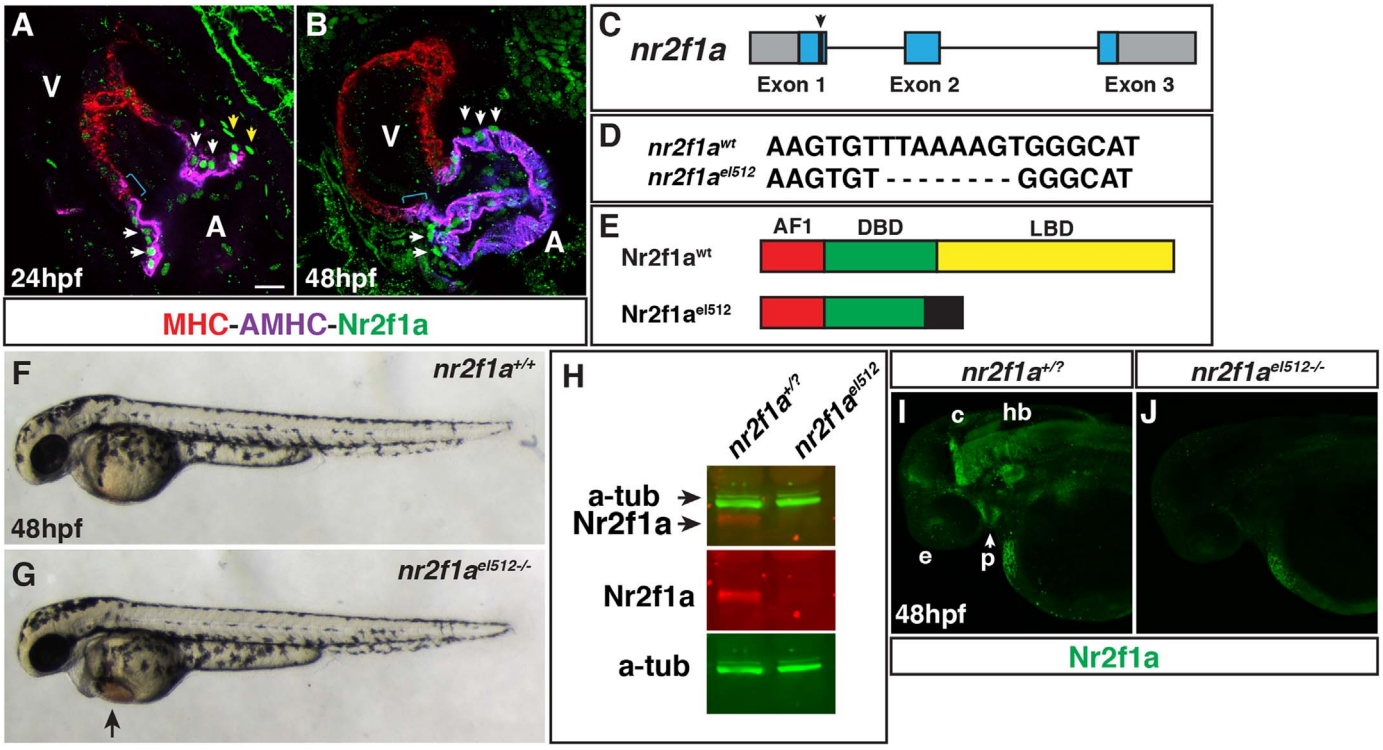

Fig. 1. Nr2f1a is expressed in ACs and generation of a *nr2f1a* mutant allele. (A,B) IHC for MHC (red), AHMC (purple), and Nr2f1a (green) at 24 and 48 hpf. Nr2f1a^{+} nuclei in cells at the venous pole adjacent to AMHC^{+} cells (yellow arrowheads), which we propose are putatively atrial progenitors. Expression in nuclei of ACs (white arrows). Blue brackets indicate AMHC^{+} region devoid of Nr2f1^{+} nuclei. Images are Z-stacks of confocal sections. V indicates ventricle and A indicates atrium in all figures. Scale bar indicates 10 μm in A,B. ≥ 10 hearts were examined at each stage. (C) Schematic of deletion in *nr2f1a* exon 1 from the TALENs. (D) Sequence of the 8-bp deletion in the *nr2f1a^{el512}* mutant allele. (E) Schematic indicating the predicted truncation caused by the deletion. Activation domain – AF1 (red), DNA-binding domain – DBD (green), Ligand binding domain – LBD (yellow). Black indicates amino acids after the protein goes out of frame. (F,G) WT and *nr2f1a $^{el512-/-}$* mutant embryos at 48 hpf. (H) Western blot indicating that Nr2f1a protein is lost in *nr2f1a* mutants. (I,J) Confocal images of whole mount IHC indicating Nr2f1a protein is expressed in the same anatomical structure as shown previously with ISH (Love and Prince, 2012) and is lost in *nr2f1a* mutants. Images are the dorsolateral with anterior left. e – eyes, p – pharyngeal (arrow in I), c – cerebellum, hb –hindbrain. > 20 wt sibling and *nr2f1a* mutant embryos were examined.

methods. Monoclonal anti-α-tubulin (T 6199, Sigma) was used as a loading control. LI-COR IRDye® 680LT Donkey anti-rabbit secondary was used for the anti-Nr2f1a antibody. LI-COR IRDye® 800CW Donkey anti-mouse secondary was used for the anti-α-tubulin. Blots were imaged using an Odyssey CLx LI-COR imager.

2.7. Zebrafish immunohistochemistry (IHC) and cardiomyocyte counting

IHC of hearts and for counting cardiomyocytes were performed as previously described (Waxman et al., 2008). Embryos were fixed for 1 h at room temperature in 1% formaldehyde in PBS, followed by washing 1X in PBS, 2X in 0.2% saponin/1X PBS, and blocking with 0.2% saponin/10%sheep serum/1X PBS (Saponin blocking solution) for one hour. AMHC (Atrial myosin heavy chain; S46) and MHC (sarcomeric myosin heavy chain; MF20) primary antibodies (University of Iowa Developmental Studies Hybridoma Bank) were incubated at 1:10 in Saponin blocking solution. Rabbit polyclonal anti-DsRed antibody (Clontech) was used at a 1:1000 dilution. Nr2f1a antibody was used at 1:100. Secondary antibodies anti-mouse IgG1-FITC (Southern Biotech), anti-mouse IgG2b-TRITC (Southern Biotech), anti-rabbit IgG-TRITC (Southern Biotech), anti-rabbit IgG(H+L) Alexa Fluor® 488 (Southern Biotech), and anti-mouse IgG1 DyLight™ 405 (BioLegend) were used at dilutions of 1:100. A Zeiss M2BioV12 Stereo microscope was used to image hearts with AHMC/MHC and DsRed/MHC IHC. A Nikon A1 inverted microscope was used to image Nr2f1a/MHC IHC.

For IHC of ECs, embryos were fixed in 4% formaldehyde overnight at 4 °C, followed by dehydration in a methanol series at −20 °C. Embryos were washed in 1X PBS/0.1% Tween-20 (PBST) then PBST/1%DMSO/0.3% Triton-X for 20 min. Embryos were blocked in PBST/10% sheep serum, followed by washes and application of the secondary antibody. Alcama/Zn8/DmGrasp (DHSB) was used at 1:10. Secondary antibody anti-mouse IgG1 Alexa Fluor® 488 (Southern Biotech) was used at 1:100. Embryos were mounted for confocal imaging by cutting the tail off with forceps, then placing the embryo downward with the heart facing the coverslip. 0.6% low melting point agar was placed on top and allowed to solidify before imaging. EC cells were counted using the cell membrane labeling of Alcama antibody.

2.8. Dorsomorphin and LDN193189 treatments

Embryos from *nr2f1a$^{+/-}$;myl7: DsRed2-NLS* adult crosses were treated with 10 μM Dorsomorphin or 10 μM LDN193189 (Sigma) diluted from a 10 mM stocks in DMSO beginning at the 20 s stage. Embryos were treated through 72 hpf when they were sorted, processed for IHC, imaged with confocal microscopy, and analyzed as above.

2.9. Kaede photoconversion analysis

Photoconversion of Kaede, imaging, and analysis were performed as previously reported (Rydeen and Waxman, 2016) with the following modifications. Embryos from crosses of *nr2f1a+/-; myl7: kaede* hemizygous fish were collected and transferred to embryo water (without methylene blue). At 30 hpf, the embryos were exposed to UV light for 30 min using a DAPI filter on a Zeiss M2BioV12 Stereo microscope. At 48 hpf, *nr2f1a* mutant and their WT sibling embryos were sorted, anesthetized, and gently compressed between two coverslips. The hearts were imaged with a Nikon A1 inverted confocal microscope. The areas of green^{+}/red^{-} cardiomyocytes were determined by subtracting the amount of red fluorescence (earlier differentiating cardiomyocytes) from the green fluorescence (later differentiating

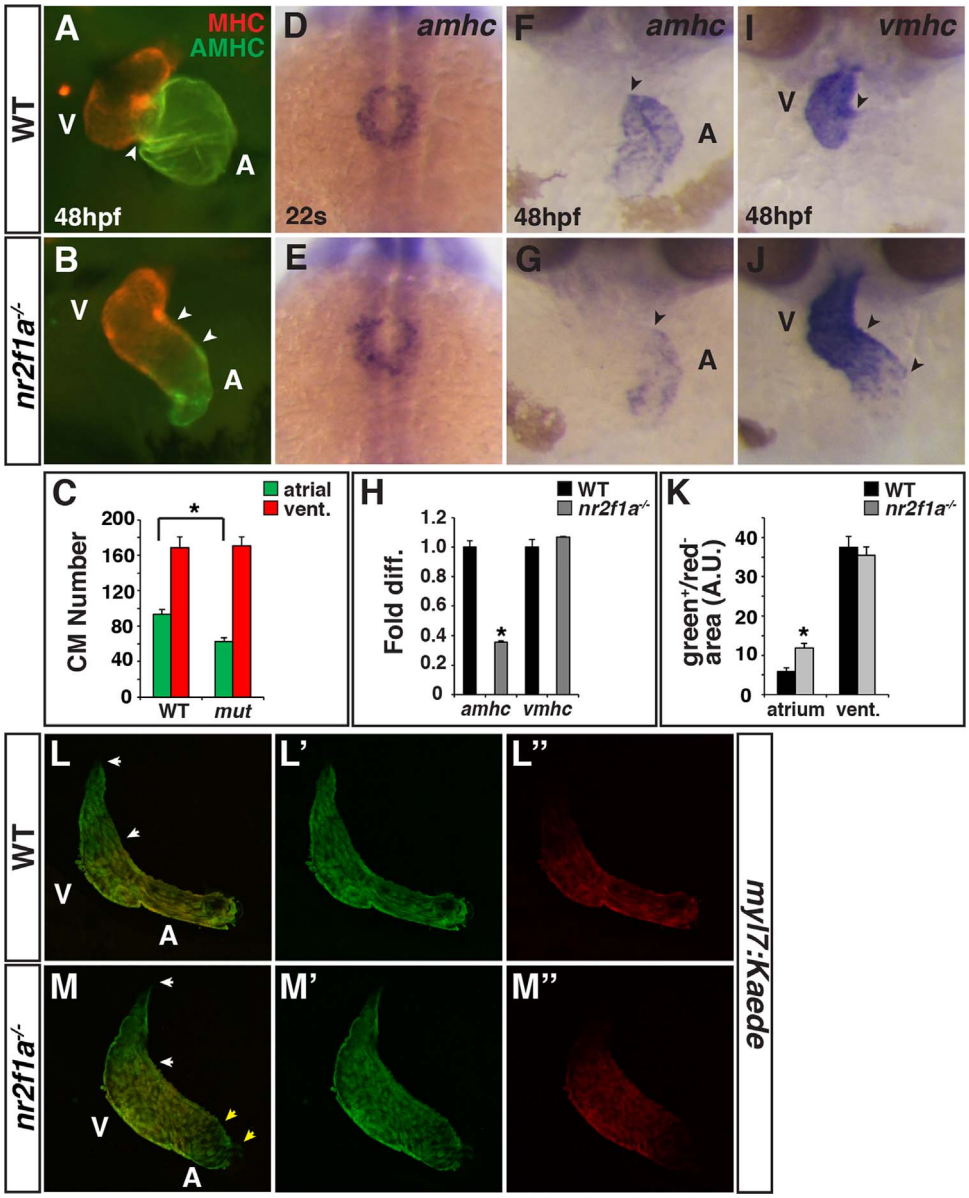

Fig. 2. *Nr2f1a* mutants have smaller atria. (A,B) IHC for MHC (red) and AMHC (green). Sharp border between MHC and AMHC in WT embryos (arrowhead in A). Diffuse border of AMHC expression (arrowheads in B). (C) Number of ACs and VCs in WT sibling (n = 12) and *nr2f1a* mutant (n = 14) embryos. (D,E) ISH for *amhc* at the 22 s stage. Images are dorsal views with anterior up. (F,G) ISH for *amhc* at 48 hpf. Border of expression (arrowheads). (H) RT-qPCR for *amhc* and *vmhc* in WT sibling and *nr2f1a* mutant embryos. (I,J) ISH for *vmhc* at 48 hpf. Distinct border of expression (arrowhead in I). Expansion and diffuse border of expression (arrowheads in J). Images in F,G,I,J are frontal views. > 20 embryos per condition were examined for A,B,D,E,F,G,I,J. (K) Amount of green$^+$/red$^-$ cells (area) at the venous (atrium) and arterial (ventricular) poles in WT and *nr2f1a* mutant embryos. (L-M″) Confocal images of hearts depicting the addition of differentiating cells (green$^+$/red$^-$ cells) at the venous and arterial poles (yellow and white arrowheads, respectively). Asterisks indicates significant difference ($P < 0.05$) in all figures.

cardiomyocytes) in two-color images at both arterial and venous poles using ImageJ (Schneider et al., 2012).

2.10. Statistical analysis

For comparisons between two conditions (Fig. 2 and Fig. 3) Student's *t*-test was used. For comparison between 4 conditions ANOVA with Tukey's test was used (Fig. 4). $P < 0.05$ was considered statistically significant for all comparisons.

3. Results

3.1. Nr2f1a is expressed in ACs

Nr2f1 is expressed in ACs of humans and mice similar to Nr2f2 (Devalla et al., 2015; Li et al., 2016). However, zebrafish Nr2f2 is not required for early heart development (van Impel et al., 2014). Therefore, we wanted to determine if the paralog *nr2f1a* is expressed in ACs of zebrafish. We examined Nr2f1a protein expression using an antibody that was generated to peptide fragments within the Nr2f1a N-terminus (Fig. S1 and Section 2). These peptides were used because the N-terminus has the least amount of conservation between Nr2f1a and other zebrafish Nr2f family members (Fig. S1). Examining Nr2f1a in the nascent heart tube at 24 hpf with IHC and confocal microscopy, we found that it was already restricted to nuclei of ACs and cells adjacent to the atrial venous pole that were not expressing the atrial marker AHMC (Fig. 1A), which we postulate may be atrial progenitors. Through 48 hpf, Nr2f1a maintained expression in ACs (Fig. 1B), but became progressively less visible in cells adjacent to the venous pole. Although Nr2f2 has been reported in endocardial cells, we did not detect Nr2f1a within endocardial cells (Fig. 1A,B). Thus, we find that Nr2f1a is specifically expressed within differentiating ACs and cells

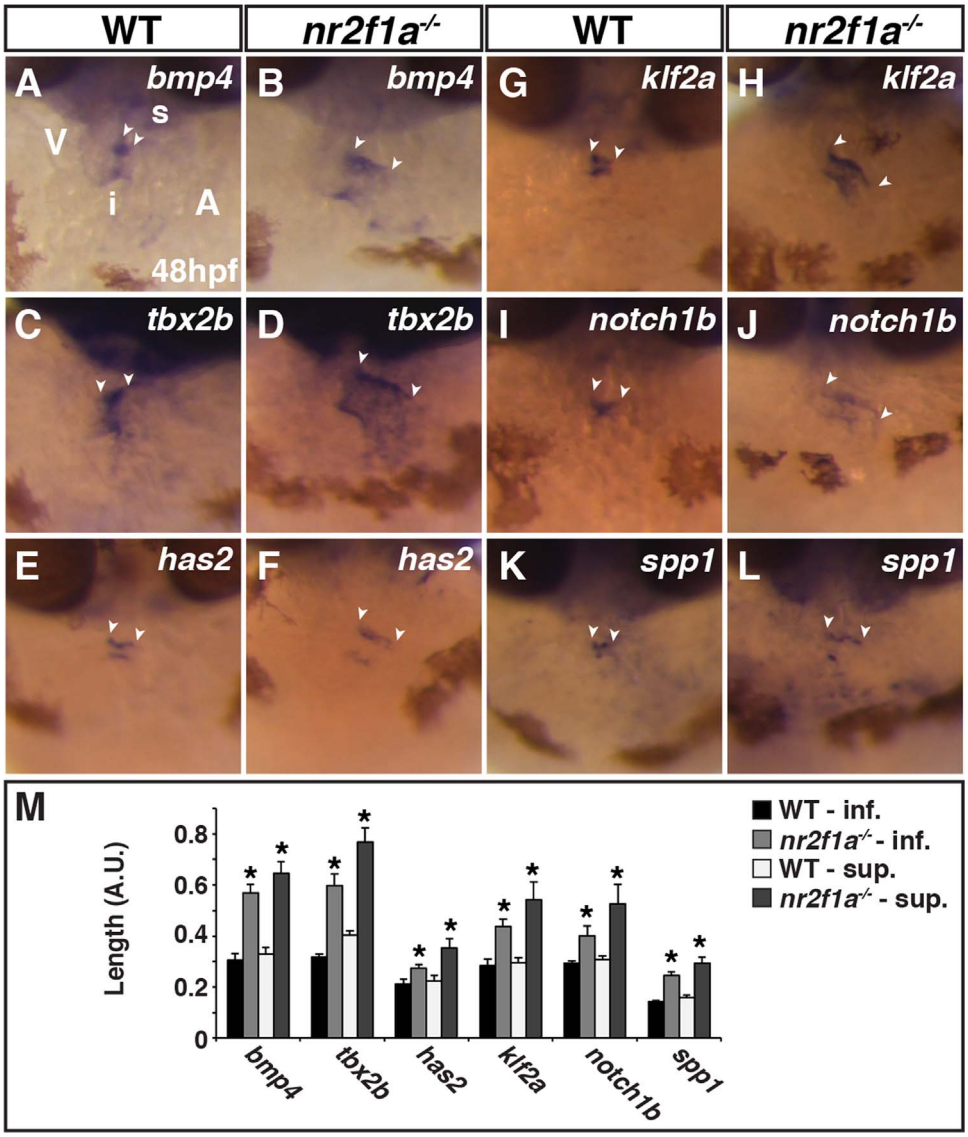

Fig. 3. AVC markers are expanded in *nr2f1a* mutant hearts. (A-L) ISH for *bmp4* (A,B), *tbx2b* (C,D), *has2* (E,F), *klf2a* (G,H), *notch1b* (I,J), and *spp1* (K,L) in WT and *nr2f1a* mutant embryos. Images are frontal views with dorsal up. The relative position of the ventricle and atrium is the same in all images. Arrowheads indicate the length of expression on the superior side (s) of the AVC, which is adjacent to the inner curvature of the ventricle. Inferior side (i) of the AVC is adjacent to the outer curvature of the ventricle. (M) Length measurements of marker expression in the AVC. (WT *bmp4* n = 7, *nr2f1a*$^{-/-}$ *bmp4* n = 7, WT *tbx2b* n = 10, *nr2f1a*$^{-/-}$ *tbx2b* n = 10, WT *has* n = 7, *nr2f1a*$^{-/-}$ *has* n = 7, WT *klf2a* n = 6, *nr2f1a*$^{-/-}$ *klf2a* n = 6, WT *notch1b* n = 5, *nr2f1a*$^{-/-}$ *notch1b* n = 5, WT *spp1* n = 9, *nr2f1a*$^{-/-}$ *klf2a* n = 9.).

adjacent to the venous atrium that we postulate are putative AC progenitors.

3.2. *Nr2f1a is required for AC differentiation*

To determine if Nr2f1a is required for proper atrial development in zebrafish embryos, we generated multiple *nr2f1a* alleles using TALENs and CRISPR/Cas9 (Fig. 1C,D and Fig. S2A,B) (Joung and Sander, 2013; Talbot and Amacher, 2014). The alleles examined cause truncations that eliminate the ligand binding domain (Fig. 1E and Fig. S2C), gave identical overt phenotypes (Fig. 1F,G and Fig. S2D,E), showed loss of Nr2f1a protein (Fig. 1H-J), and failed to complement each other (data not shown). Therefore, the *nr2f1a* alleles were used interchangeably for experiments and henceforth are referred to as *nr2f1a* mutants.

Although it was difficult to identify *nr2f1a* mutants at earlier stages, we found that they develop overt pericardial edema by 48 hpf (Fig. 1F,G and Fig. S2D,E). Examination of the hearts from *nr2f1a* mutants with IHC revealed aberrant morphology, with the atria typically appearing smaller (Fig. 2A,B and Fig. S3A,B). Importantly, while these phenotypes are reminiscent of the atria described in global Nr2f2 KO mice (Pereira et al., 1999), the cause(s) of the dysmorphic, smaller atria occurring in the Nr2f2 KO mice has not been reported. Interestingly, counting the cardiomyocytes, using the *myl7: DsRed-NLS* transgene (Fig. S3A,B) (Mably et al., 2003), revealed a specific decrease in ACs of *nr2f1a* mutants, without affecting VC number (Fig. 2C). Examination of the atrial differentiation marker *atrial myosin heavy chain* (*amhc* aka *myh6*) at the 22 somite (s) stage via ISH did not reveal any obvious differences between *nr2f1a* mutants and their wild-type (WT) siblings (Fig. 2D,E), suggesting early specification and differentiation of ACs is likely not affected in *nr2f1a* mutants. However, ISH and RT-qPCR both revealed decreased *amhc* expression by 48 hpf relative to WT siblings (Fig. 2F-H), supporting a requirement for Nr2f1a in promoting addition of ACs later and/or enhancing atrial differentiation. In contrast to counting cardiomyocytes, which differentiates ACs and VCs using AMHC^{+} protein expression and showed no effect on VC number (Fig. 2A-C and Fig. 3SA,B), we observed an expansion of the VC differentiation marker *ventricular myosin heavy chain (vmhc)* (Fig. 2I,J). Although we also did not

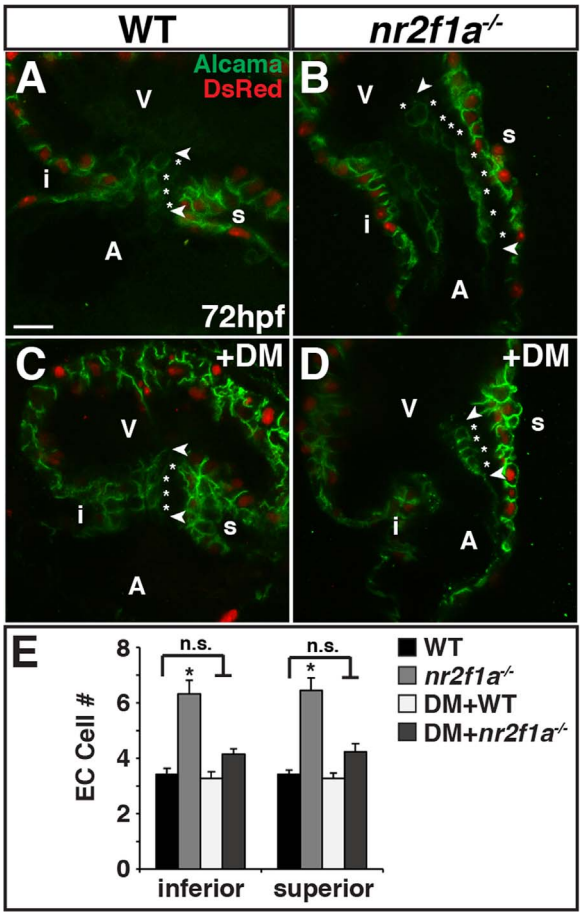

Fig. 4. Nr2f1a functions upstream of Bmp signaling to restrict ECs. (A-D) IHC of hearts from *myl7: DsRed-NLS* WT, *nr2f1a* mutant, WT DM-treated, and *nr2f1a* mutant DM-treated embryos for Alcama (green) and DsRed (myocardial nuclei – red). Images are frontal views of confocal stacks. Length of ECs (arrowheads). Individual EC cells (asterisks). Scale bar indicates 10 μm in A-D. (E) Mean EC number from inferior and superior valve sides in WT (n = 12), *nr2f1a* mutant (n = 9), WT DM-treated (n = 11), and *nr2f1a* mutant DM-treated (n = 13) embryos.

observe a quantitative difference in *vmhc* expression with RT-qPCR at this stage (Fig. 2H), a caveat of this analysis is that it was performed on whole embryos and *vmhc* is also expressed in the somites. However, because *vmhc* and *amhc* expression overlap within cells of the less differentiated AVC (Auman et al., 2007; Pradhan et al., 2017), we postulate the expansion of *vmhc* alone within the heart may not necessarily reflect an expansion of differentiated VCs into the atrium, even though it has traditionally been considered solely a marker of VC differentiation. Cumulatively, these data support that the smaller atria in *nr2f1a* mutants are due to reduced AC number, which is not from a direct expansion of VCs at the expense of ACs in *nr2f1a* mutants, at least through 48 hpf.

In mammals, the atria are largely derived from later differentiating, posterior second heart field (SHF) progenitors (Galli et al., 2008). While the contribution of later differentiating venous cardiomyocytes is not as dramatic in zebrafish, there is some accrual of ACs at the venous pole of the heart (de Pater et al., 2009). Because we observe Nr2f1a-expressing cells adjacent to the venous atrium in the nascent heart tube, but progressively fewer later, this observation implied that Nr2f1a may be affecting the differentiation of these venous progenitor cells into ACs. We assessed the temporal differentiation of cardiomyocytes at the venous pole in *nr2f1a* mutants using the *myl7: Kaede* transgene (de Pater et al., 2009). Kaede-expressing cardiomyocytes from adult *nr2f1a*$^{+/-}$ crosses were converted from green to red in 30 hpf embryos, followed by sorting of *nr2f1a* mutant and WT sibling embryos and imaging at 48 hpf. Interestingly, we found that there was an increased amount of green^{+}/red^{-} cells at the venous pole of *nr2f1a* mutants compared to their WT siblings (Fig. 2K-M″). In the same hearts, we did not observe a difference in the amount of green^{+}/red^{-} VCs adding to the outflow tract (Fig. 2K-M″). Altogether, these results suggest that reduced and/or delayed rate of differentiation at the venous pole contributes to the deficit of ACs in *nr2f1a* mutants.

3.3. Nr2f1a is required to restrict AVC markers

The loss of ACs can explain some aspects of the smaller, dysmorphic atria in *nr2f1a* mutants. However, we also found that the border between the ACs (AMHC^{+}) and VCs (AMHC^{-}) cells was more diffuse in *nr2f1a* mutant hearts (Fig. 2A,B and Fig. 3SA,B). Together with the observation that there is an expansion of *vmhc* expression in *nr2f1a* mutants into the atria (Fig. 2I,J), but not a difference in VC number (Fig. 2C), we postulated that patterning of the AVC may be disrupted in *nr2f1a* mutants. A well-established conserved hierarchy of signals determine the AVC in vertebrates (reviewed in Haack and Abdelilah-Seyfried (2016)). In zebrafish, at the border of the atrial and ventricular chambers, the AVC myocardium is established by Bone morphogenetic protein 4 (Bmp4) signaling, which lies upstream of the transcription factor Tbx2b and maintains a less-differentiated cardiomyocyte state (de Pater et al., 2012). Signals from the myocardium are relayed to the adjacent AVC endocardium, initiating expression of factors including *hyaluronan synthase 2 (has2)* and the transcription factor *Kruppel-like factor 2a (klf2a)* that ultimately permit expression of *notch1b* and valve differentiation, as indicated by the marker *secreted phosphoprotein 1 (spp1)*. Examining these AVC markers in *nr2f1a* mutants, we found that all were dramatically expanded into the atria compared to WT siblings (Fig. 3A-M), which was similar to the expansion of *vmhc* expression (Fig. 2I,J). Next, to examine if the expansion of these AVC markers in *nr2f1a* mutants results in an expansion of the EC cells, as would be predicted, we used Alcama (aka Dm-grasp) IHC at 72 hpf (Beis et al., 2005; Smith et al., 2011). Indeed, we found that the number of EC cells was almost doubled for both the superior and inferior cushions (Fig. 4A,B,E).

Bmp signaling is required within the AVC myocardium to repress cardiomyocyte differentiation after its initial role in promoting cardiomyocytes specification (de Pater et al., 2012; Haack and Abdelilah-Seyfried, 2016). We find that AMHC^{+} cells adjacent to the ventricle appear to lack Nr2f1a (Fig. 1A,B), suggesting Nr2f1a expression extends up to the border of the AVC, and that *nr2f1a* mutants have an expanded AVC (Fig. 3). Therefore, we posited that Nr2f1a lies upstream of Bmp signaling to restrict valve development. To test this hypothesis, we treated embryos from *nr2f1a*$^{+/-}$ crosses with the Bmp signaling inhibitor Dorsomorphin (DM) (Hao et al., 2008) beginning at the 20 s stage, since this is when BMP was found to repress cardiomyocyte differentiation (de Pater et al., 2012). Remarkably, although the atria of DM-treated *nr2f1a* mutant embryos were still dysmorphic, we found that inhibition of BMP signaling was able to restore their number of ECs (Fig. 4C-E). A similar restoration of ECs was observed in the *nr2f1a* mutants when treating with the BMP signaling inhibitor LDN193189 (Fig. S4) (Cuny et al., 2008). However, despite the ability to restore EC number, BMP inhibition did not rescue the number of ACs in *nr2f1a* mutants (Fig. S3C). Therefore, these data support that within the atrial myocardium Nr2f1a is necessary to limit BMP signaling and the size of the AVC.

4. Discussion

4.1. Conserved functions of Nr2f factors in vertebrate atrial development and disease

Recent data has indicated that Nr2f1 is expressed in the atria of mice and hESC-derived ACs similar to Nr2f2 (Devalla et al., 2015; Li

et al., 2016). Depletion of Nr2f1 in stem cell-derived human atrial cells indicated a potentially overlapping function with Nr2f2 promoting atrial differentiation (Devalla et al., 2015), although the importance of Nr2f1 in mouse atrial development has not been reported. While a recent study using morpholinos to deplete Nr2f1a in zebrafish embryos suggested that it is required for vascular development (Wu et al., 2014), similar to the role of Nr2f2 in mammalian endothelial cells (Pereira et al., 1999; You et al., 2005), that study did not analyze requirements for Nr2f1a in the heart. However, while not the focus of this study, we do not find overt vascular defects in *nr2f1a* mutants (data not shown). Our data examining multiple *nr2f1a* mutant alleles support the hypothesis that Nr2f1a functions to promote atrial development and differentiation in a manner equivalent to Nr2f2 in mammals. Thus, we surmise that observations from our study represent previously unrecognized, conserved mechanisms of the Nr2f family that significantly extend studies of Nr2f2 in atrial development of mammals.

Foremost, the previous study of global *Nr2f2* KOs did not reveal the causes of the morphological smaller atria and sinus venous (Pereira et al., 1999). Because we find that the smaller atria in zebrafish *nr2f1a* mutants are partially due to reduced and delayed AC differentiation at the venous pole, we propose that the smaller atria in *Nr2f2* mouse mutants are also secondary to decreased AC number derived from a failure of posterior SHF cells to accrue and differentiate. Conditional KOs using a *Myh6-cre* to deplete Nr2f2 in cardiomyocytes beginning at E9.5 demonstrated Nr2f2 promotes the differentiation and maintenance of atrial identity at the expense of ventricular identity upstream of *Irx4* and *Hey2* (Wu et al., 2013). In contrast to this observation, our cardiomyocyte counts and quantitative expression data do not support that Nr2f1a promotes atrial identity at the expense of ventricular identity, at least during initial stages of cardiac chamber development in zebrafish. We do observe a visible expansion of *vmhc,* which traditionally is thought to mark differentiated VCs, within the hearts of *nr2f1a* mutants. However, we posit that this expansion reflects a general expansion of the AVC, since we find a similar expansion of the other canonical AVC markers examined and do not find an increase in the $AMHC^-$ VCs that complements the loss of $AMHC^+$ cardiomyocytes in *nr2f1a* mutants. One interpretation of the contrasting observations reported here and by Wu et al. (2013) is that we each have identified different temporal requirements of Nr2f factors in vertebrate atrial development. We propose that our analysis has uncovered a previously overlooked requirement for Nr2f proteins in establishing fully differentiated ACs at the atria-AVC border, while the conditional mouse Nr2f2 KO study revealed a later role in maintenance of atrial identity at the expense of ventricular identity (Wu et al., 2013). Moreover, in contrast to the global mouse *Nr2f2* KOs and the zebrafish *nr2f1a* mutants, the atrial chambers in the conditional *Nr2f2* KOs were larger, not smaller, reflecting the later acquisition of VC characteristics and enhanced proliferation. Thus, the atrial phenotypes in the global vs conditional Nr2f protein KOs further highlight the different requirements of Nr2f transcription factors within atrial development.

Importantly, AVC defects were not reported in the global or conditional Nr2f2 KOs (Wu et al., 2013). Thus, despite the cardiomyocyte fate transformations and morphological defects observed, these previous studies did not reveal potential causes for the AVSDs associated with *NR2F2* mutations in humans. Conditional *Nr2f2* KO within the endocardium of mice using the *Tie1-cre* illustrated endocardial-mesenchymal transition defects within the ECs due to an expansion of Notch (Lin et al., 2012). However, it is unlikely that the valve defects from endocardial Nr2f2 depletion can explain AVSDs. Our data point to a role for Nr2f factors functioning within the differentiating atrial myocardium at the top of the AVC developmental hierarchy to restrict Bmp signaling that concomitantly establishes both atrial chamber and AVC/valve size. Interestingly, even though *bmp4* is also expressed at the venous pole (de Pater et al., 2009), our data suggest that Nr2f1a function at the venous pole is independent of Bmp signaling. While other factors have been found to restrict AVC expansion into the ventricle (Beis et al., 2005; Garrity et al., 2002; Just et al., 2011; Rutenberg et al., 2006; Smith et al., 2011; Totong et al., 2011), to our knowledge Nr2f1a is the first factor found to restrict AVC specification within the atrium and lead to differentiation of the EC cells, as indicated by *spp1* expression. Therefore, we speculate that the *NR2F2*-associated AVSDs in humans may in part be due to a failure to restrict the size of the AVC. Altogether, our data indicate that in zebrafish Nr2f1a coordinates atrial chamber and AVC size through both BMP signaling-independent and -dependent mechanisms, providing insight into the conserved requirements of Nr2f transcription factors in vertebrate chamber development and, potentially, unknown etiology of AVSDs associated with *NR2F2* mutations in humans.

Acknowledgements

We thank J. Schumacher for *spp1* probe and LDN193189, and K. Targoff for helpful discussion and comments regarding the manuscript.

Author contributions

T.B.D., T.E.D., and J.S.W. designed the studies; T.B.D., P.R., Y.C.S., J.T.G., A.B.R., T.E.D., and J.S.W. performed experiments; T.E.D., P.R., L.A.B., and J.G.C generated reagents; T.B.D., P.R., Y.C.S., J.T.G., A.B.R., and J.S.W. analyzed data. T.B.D., T.E.D., Y.C.S., L.A.B., and J.S.W. wrote the manuscript with guidance and input from all authors.

Competing interests

The authors declare no competing interests.

Funding

This work was supported by grants from the National Institutes of Health [R01HL112893 and R01HL137766 to J.S.W.; R01DE018405 to J.G.C.; K99DE026239 to L.A.B.] and American Heart Association [15PRE25090070 to A.B.R. and 17PRE33661080 to Y.C.S.].

Appendix A. Supplementary material

Supplementary data associated with this article can be found in the online version at http://dx.doi.org/10.1016/j.ydbio.2017.11.010.

References

Abu-Issa, R., Kirby, M.L., 2008. Patterning of the heart field in the chick. Dev. Biol. 319, 223–233.

Al Turki, S., Manickaraj, A.K., Mercer, C.L., Gerety, S.S., Hitz, M.P., Lindsay, S., D'Alessandro, L.C., Swaminathan, G.J., Bentham, J., Arndt, A.K., Low, J., Breckpot, J., Gewillig, M., Thienpont, B., Abdul-Khaliq, H., Harnack, C., Hoff, K., Kramer, H.H., Schubert, S., Siebert, R., Toka, O., Cosgrove, C., Watkins, H., Lucassen, A.M., O'Kelly, I.M., Salmon, A.P., Bu'lock, F.A., Granados-Riveron, J., Setchfield, K., Thornborough, C., Brook, J.D., Mulder, B., Klaassen, S., Bhattacharya, S., Devriendt, K., Fitzpatrick, D.F., Consortium, U.K., Wilson, D.I., Mital, S., Hurles, M.E., 2014. Rare variants in NR2F2 cause congenital heart defects in humans. Am. J. Hum. Genet. 94, 574–585.

Auman, H.J., Coleman, H., Riley, H.E., Olale, F., Tsai, H.J., Yelon, D., 2007. Functional modulation of cardiac form through regionally confined cell shape changes. PLoS Biol. 5, e53.

Barth, A.S., Merk, S., Arnoldi, E., Zwermann, L., Kloos, P., Gebauer, M., Steinmeyer, K., Bleich, M., Kaab, S., Pfeufer, A., Uberfuhr, P., Dugas, M., Steinbeck, G., Nabauer, M., 2005. Functional profiling of human atrial and ventricular gene expression. Pflug. Arch. 450, 201–208.

Beis, D., Bartman, T., Jin, S.W., Scott, I.C., D'Amico, L.A., Ober, E.A., Verkade, H., Frantsve, J., Field, H.A., Wehman, A., Baier, H., Tallafuss, A., Bally-Cuif, L., Chen, J.N., Stainier, D.Y., Jungblut, B., 2005. Genetic and cellular analyses of zebrafish atrioventricular cushion and valve development. Development 132, 4193–4204.

Bruneau, B.G., Bao, Z.Z., Tanaka, M., Schott, J.J., Izumo, S., Cepko, C.L., Seidman, J.G., Seidman, C.E., 2000. Cardiac expression of the ventricle-specific homeobox gene Irx4 is modulated by Nkx2-5 and dHand. Dev. Biol. 217, 266–277.

Bruneau, B.G., Bao, Z.Z., Fatkin, D., Xavier-Neto, J., Georgakopoulos, D., Maguire, C.T., Berul, C.I., Kass, D.A., Kuroski-de Bold, M.L., de Bold, A.J., Conner, D.A., Rosenthal,

N., Cepko, C.L., Seidman, C.E., Seidman, J.G., 2001. Cardiomyopathy in Irx4-deficient mice is preceded by abnormal ventricular gene expression. Mol. Cell. Biol. 21, 1730–1736.
Cuny, G.D., Yu, P.B., Laha, J.K., Xing, X., Liu, J.F., Lai, C.S., Deng, D.Y., Sachidanandan, C., Bloch, K.D., Peterson, R.T., 2008. Structure-activity relationship study of bone morphogenetic protein (BMP) signaling inhibitors. Bioorg. Med. Chem. Lett. 18, 4388–4392.
D'Aniello, E., Rydeen, A.B., Anderson, J.L., Mandal, A., Waxman, J.S., 2013. Depletion of retinoic acid receptors initiates a novel positive feedback mechanism that promotes teratogenic increases in retinoic acid. PLoS Genet. 9, e1003689.
DeLaughter, D.M., Bick, A.G., Wakimoto, H., McKean, D., Gorham, J.M., Kathiriya, I.S., Hinson, J.T., Homsy, J., Gray, J., Pu, W., Bruneau, B.G., Seidman, J.G., Seidman, C.E., 2016. Single-cell resolution of temporal gene expression during heart development. Dev. Cell 39, 480–490.
Devalla, H.D., Schwach, V., Ford, J.W., Milnes, J.T., El-Haou, S., Jackson, C., Gkatzis, K., Elliott, D.A., Chuva de Sousa Lopes, S.M., Mummery, C.L., Verkerk, A.O., Passier, R., 2015. Atrial-like cardiomyocytes from human pluripotent stem cells are a robust preclinical model for assessing atrial-selective pharmacology. EMBO Mol. Med. 7, 394–410.
Devine, W.P., Wythe, J.D., George, M., Koshiba-Takeuchi, K., Bruneau, B.G., 2014. Early patterning and specification of cardiac progenitors in gastrulating mesoderm. eLife 3.
Foglia, M.J., Cao, J., Tornini, V.A., Poss, K.D., 2016. Multicolor mapping of the cardiomyocyte proliferation dynamics that construct the atrium. Development 143, 1688–1696.
Galli, D., Dominguez, J.N., Zaffran, S., Munk, A., Brown, N.A., Buckingham, M.E., 2008. Atrial myocardium derives from the posterior region of the second heart field, which acquires left-right identity as Pitx2c is expressed. Development 135, 1157–1167.
Garcia-Martinez, V., Schoenwolf, G.C., 1993. Primitive-streak origin of the cardiovascular system in avian embryos. Dev. Biol. 159, 706–719.
Garrity, D.M., Childs, S., Fishman, M.C., 2002. The heartstrings mutation in zebrafish causes heart/fin Tbx5 deficiency syndrome. Development 129, 4635–4645.
Gupta, V., Poss, K.D., 2012. Clonally dominant cardiomyocytes direct heart morphogenesis. Nature 484, 479–484.
Haack, T., Abdelilah-Seyfried, S., 2016. The force within: endocardial development, mechanotransduction and signalling during cardiac morphogenesis. Development 143, 373–386.
Hao, J., Daleo, M.A., Murphy, C.K., Yu, P.B., Ho, J.N., Hu, J., Peterson, R.T., Hatzopoulos, A.K., Hong, C.C., 2008. Dorsomorphin, a selective small molecule inhibitor of BMP signaling, promotes cardiomyogenesis in embryonic stem cells. PLoS One 3, e2904.
Jao, L.E., Wente, S.R., Chen, W., 2013. Efficient multiplex biallelic zebrafish genome editing using a CRISPR nuclease system. Proc. Natl. Acad. Sci. USA 110, 13904–13909.
Joung, J.K., Sander, J.D., 2013. TALENs: a widely applicable technology for targeted genome editing. Nat. Rev. Mol. Cell Biol. 14, 49–55.
Just, S., Berger, I.M., Meder, B., Backs, J., Keller, A., Marquart, S., Frese, K., Patzel, E., Rauch, G.J., Tubingen Screen, C., Katus, H.A., Rottbauer, W., 2011. Protein kinase D2 controls cardiac valve formation in zebrafish by regulating histone deacetylase 5 activity. Circulation 124, 324–334.
Keegan, B.R., Meyer, D., Yelon, D., 2004. Organization of cardiac chamber progenitors in the zebrafish blastula. Development 131, 3081–3091.
Koibuchi, N., Chin, M.T., 2007. CHF1/Hey2 plays a pivotal role in left ventricular maturation through suppression of ectopic atrial gene expression. Circ. Res. 100, 850–855.
Li, G., Xu, A., Sim, S., Priest, J.R., Tian, X., Khan, T., Quertermous, T., Zhou, B., Tsao, P.S., Quake, S.R., Wu, S.M., 2016. Transcriptomic profiling maps anatomically patterned subpopulations among single embryonic cardiac cells. Dev. Cell 39, 491–507.
Lin, F.J., You, L.R., Yu, C.T., Hsu, W.H., Tsai, M.J., Tsai, S.Y., 2012. Endocardial cushion morphogenesis and coronary vessel development require chicken ovalbumin upstream promoter-transcription factor II. Arterioscler. Thromb. Vasc. Biol. 32, e135–e146.
Love, C.E., Prince, V.E., 2012. Expression and retinoic acid regulation of the zebrafish nr2f orphan nuclear receptor genes. Dev. Dyn. 241, 1603–1615.
Mably, J.D., Mohideen, M.A., Burns, C.G., Chen, J.N., Fishman, M.C., 2003. heart of glass regulates the concentric growth of the heart in zebrafish. Curr. Biol. 13, 2138–2147.
McGrath, M.F., de Bold, A.J., 2009. Transcriptional analysis of the mammalian heart with special reference to its endocrine function. BMC Genom. 10, 254.
Oxtoby, E., Jowett, T., 1993. Cloning of the zebrafish krox-20 gene (krx-20) and its expression during hindbrain development. Nucleic Acids Res. 21, 1087–1095.
de Pater, E., Clijsters, L., Marques, S.R., Lin, Y.F., Garavito-Aguilar, Z.V., Yelon, D., Bakkers, J., 2009. Distinct phases of cardiomyocyte differentiation regulate growth of the zebrafish heart. Development 136, 1633–1641.
de Pater, E., Ciampricotti, M., Priller, F., Veerkamp, J., Strate, I., Smith, K., Lagendijk, A.K., Schilling, T.F., Herzog, W., Abdelilah-Seyfried, S., Hammerschmidt, M., Bakkers, J., 2012. Bmp signaling exerts opposite effects on cardiac differentiation. Circ. Res. 110, 578–587.
Pereira, F.A., Qiu, Y., Zhou, G., Tsai, M.J., Tsai, S.Y., 1999. The orphan nuclear receptor COUP-TFII is required for angiogenesis and heart development. Genes Dev. 13, 1037–1049.
Pradhan, A., Zeng, X.I., Sidhwani, P., Marques, S.R., George, V., Targoff, K.L., Chi, N.C., Yelon, D., 2017. FGF signaling enforces cardiac chamber identity in the developing ventricle. Development 144, 1328–1338.
Reifers, F., Bohli, H., Walsh, E.C., Crossley, P.H., Stainier, D.Y., Brand, M., 1998. Fgf8 is mutated in zebrafish acerebellar (ace) mutants and is required for maintenance of midbrain-hindbrain boundary development and somitogenesis. Development 125, 2381–2395.
Rutenberg, J.B., Fischer, A., Jia, H., Gessler, M., Zhong, T.P., Mercola, M., 2006. Developmental patterning of the cardiac atrioventricular canal by Notch and hairy-related transcription factors. Development 133, 4381–4390.
Rydeen, A., Voisin, N., D'Aniello, E., Ravisankar, P., Devignes, C.S., Waxman, J.S., 2015. Excessive feedback of Cyp26a1 promotes cell non-autonomous loss of retinoic acid signaling. Dev. Biol. 405, 47–55.
Rydeen, A.B., Waxman, J.S., 2016. Cyp26 enzymes facilitate second heart field progenitor addition and maintenance of ventricular integrity. PLoS Biol. 14, e2000504.
Sanjana, N.E., Cong, L., Zhou, Y., Cunniff, M.M., Feng, G., Zhang, F., 2012. A transcription activator-like effector toolbox for genome engineering. Nat. Protoc. 7, 171–192.
Schneider, C.A., Rasband, W.S., Eliceiri, K.W., 2012. NIH Image to ImageJ: 25 years of image analysis. Nat. Methods 9, 671–675.
Schott, J.J., Benson, D.W., Basson, C.T., Pease, W., Silberbach, G.M., Moak, J.P., Maron, B.J., Seidman, C.E., Seidman, J.G., 1998. Congenital heart disease caused by mutations in the transcription factor NKX2-5. Science 281, 108–111.
Smith, K.A., Lagendijk, A.K., Courtney, A.D., Chen, H., Paterson, S., Hogan, B.M., Wicking, C., Bakkers, J., 2011. Transmembrane protein 2 (Tmem2) is required to regionally restrict atrioventricular canal boundary and endocardial cushion development. Development 138, 4193–4198.
Smyrnias, I., Mair, W., Harzheim, D., Walker, S.A., Roderick, H.L., Bootman, M.D., 2010. Comparison of the T-tubule system in adult rat ventricular and atrial myocytes, and its role in excitation-contraction coupling and inotropic stimulation. Cell Calcium 47, 210–223.
Stainier, D.Y., Fishman, M.C., 1992. Patterning the zebrafish heart tube: acquisition of anteroposterior polarity. Dev. Biol. 153, 91–101.
Tabibiazar, R., Wagner, R.A., Liao, A., Quertermous, T., 2003. Transcriptional profiling of the heart reveals chamber-specific gene expression patterns. Circ. Res. 93, 1193–1201.
Talbot, J.C., Amacher, S.L., 2014. A streamlined CRISPR pipeline to reliably generate zebrafish frameshifting alleles. Zebrafish 11, 583–585.
Targoff, K.L., Schell, T., Yelon, D., 2008. Nkx genes regulate heart tube extension and exert differential effects on ventricular and atrial cell number. Dev. Biol. 322, 314–321.
Targoff, K.L., Colombo, S., George, V., Schell, T., Kim, S.H., Solnica-Krezel, L., Yelon, D., 2013. Nkx genes are essential for maintenance of ventricular identity. Development 140, 4203–4213.
Totong, R., Schell, T., Lescroart, F., Ryckebusch, L., Lin, Y.F., Zygmunt, T., Herwig, L., Krudewig, A., Gershoony, D., Belting, H.G., Affolter, M., Torres-Vazquez, J., Yelon, D., 2011. The novel transmembrane protein Tmem2 is essential for coordination of myocardial and endocardial morphogenesis. Development 138, 4199–4205.
van Impel, A., Zhao, Z., Hermkens, D.M., Roukens, M.G., Fischer, J.C., Peterson-Maduro, J., Duckers, H., Ober, E.A., Ingham, P.W., Schulte-Merker, S., 2014. Divergence of zebrafish and mouse lymphatic cell fate specification pathways. Development 141, 1228–1238.
Waldo, K.L., Hutson, M.R., Ward, C.C., Zdanowicz, M., Stadt, H.A., Kumiski, D., Abu-Issa, R., Kirby, M.L., 2005. Secondary heart field contributes myocardium and smooth muscle to the arterial pole of the developing heart. Dev. Biol. 281, 78–90.
Waxman, J.S., Keegan, B.R., Roberts, R.W., Poss, K.D., Yelon, D., 2008. Hoxb5b acts downstream of retinoic acid signaling in the forelimb field to restrict heart field potential in zebrafish. Dev. Cell 15, 923–934.
Wu, B.J., Chiu, C.C., Chen, C.L., Wang, W.D., Wang, J.H., Wen, Z.H., Liu, W., Chang, H.W., Wu, C.Y., 2014. Nuclear receptor subfamily 2 group F member 1a (nr2f1a) is required for vascular development in zebrafish. PLoS One 9, e105939.
Wu, S.P., Cheng, C.M., Lanz, R.B., Wang, T., Respress, J.L., Ather, S., Chen, W., Tsai, S.J., Wehrens, X.H., Tsai, M.J., Tsai, S.Y., 2013. Atrial identity is determined by a COUP-TFII regulatory network. Dev. Cell 25, 417–426.
Xin, M., Small, E.M., van Rooij, E., Qi, X., Richardson, J.A., Srivastava, D., Nakagawa, O., Olson, E.N., 2007. Essential roles of the bHLH transcription factor Hrt2 in repression of atrial gene expression and maintenance of postnatal cardiac function. Proc. Natl. Acad. Sci. USA 104, 7975–7980.
You, L.R., Lin, F.J., Lee, C.T., DeMayo, F.J., Tsai, M.J., Tsai, S.Y., 2005. Suppression of Notch signalling by the COUP-TFII transcription factor regulates vein identity. Nature 435, 98–104.